BRAIN
A JOURNAL OF NEUROLOGY

SNARE protein redistribution and synaptic failure in a transgenic mouse model of Parkinson's disease

Pablo Garcia-Reitböck,[1],* Oleg Anichtchik,[1],* Arianna Bellucci,[2] Mariangela Iovino,[1] Chiara Ballini,[3] Elena Fineberg,[1] Bernardino Ghetti,[4] Laura Della Corte,[3] PierFranco Spano,[2] George K. Tofaris,[5] Michel Goedert[6] and Maria Grazia Spillantini[1]

1 Centre for Brain Repair, Department of Clinical Neurosciences, University of Cambridge, Cambridge CB2 0PY, UK
2 Division of Pharmacology, Department of Biomedical Sciences and Biotechnologies, University of Brescia, Brescia 25123, Italy
3 Department of Preclinical and Clinical Pharmacology, University of Florence, Florence 50139, Italy
4 Department of Pathology and Laboratory Medicine, University of Indiana, Indianapolis, 46202 IN, USA
5 Department of Clinical Neurology, University of Oxford, Oxford OX3 9DU, UK
6 MRC Laboratory of Molecular Biology, Cambridge, CB2 0QH, UK

*These authors contributed equally to this work.

Correspondence to: Professor Maria Grazia Spillantini,
Cambridge Centre for Brain Repair,
Forvie Site,
Robinson Way Cambridge CB2 0PY,
UK
E-mail: mgs11@cam.ac.uk

The pre-synaptic protein α-synuclein is the main component of Lewy bodies and Lewy neurites, the defining neuropathological characteristics of Parkinson's disease and dementia with Lewy bodies. Mutations in the α-synuclein gene cause familial forms of Parkinson's disease and dementia with Lewy bodies. We previously described a transgenic mouse line expressing truncated human α-synuclein(1-120) that develops α-synuclein aggregates, striatal dopamine deficiency and reduced locomotion, similar to Parkinson's disease. We now show that in the striatum of these mice, as in Parkinson's disease, synaptic accumulation of α-synuclein is accompanied by an age-dependent redistribution of the synaptic SNARE proteins SNAP-25, syntaxin-1 and synaptobrevin-2, as well as by an age-dependent reduction in dopamine release. Furthermore, the release of FM1-43 dye from PC12 cells expressing either human full-length α-synuclein(1–140) or truncated α-synuclein(1-120) was reduced. These findings reveal a novel gain of toxic function of α-synuclein at the synapse, which may be an early event in the pathogenesis of Parkinson's disease.

Introduction

The pre-synaptic 140 amino acid protein α-synuclein is central to the aetiology and pathogenesis of Parkinson's disease, other Lewy body disorders and multiple system atrophy (Goedert, 2001). Mutations or multiplications of the α-synuclein gene cause familial forms of Parkinson's disease and dementia with Lewy bodies (Polymeropoulos *et al.*, 1997; Krüger *et al.*, 1998; Singleton *et al.*, 2003; Ibanez *et al.*, 2004; Zarranz *et al.*, 2004), and α-synuclein is the major component of Lewy bodies and Lewy neurites (Spillantini *et al.*, 1997, 1998). We previously reported the production and characterization of a transgenic mouse line, called α-syn(1-120), which expresses carboxy-terminally truncated human α-synuclein(1-120) under the control of the rat tyrosine hydroxylase promoter and in the absence of mouse α-synuclein (Tofaris *et al.*, 2006). Truncation is known to enhance aggregation of α-synuclein (Crowther *et al.*, 1998; Serpell *et al.*, 2000; Periquet *et al.*, 2007) and increased levels of truncated α-synuclein have been found in Parkinson's disease brain (Baba *et al.*, 1998; Tofaris *et al.*, 2003; Liu *et al.*, 2005). The α-syn(1-120) mice develop aggregates containing granular and filamentous α-synuclein in dopaminergic nerve cells of the substantia nigra and show a reduction in striatal dopamine, as well as motor abnormalities, in the absence of dopaminergic nerve cell death. They thus represent a model of early Parkinson's disease and can help us to understand the effects of α-synuclein on dopaminergic nerve cells prior to the onset of frank neurodegeneration. We show here that the expression of truncated or full-length α-synuclein leads to a redistribution of soluble N-ethylmaleimide sensitive fusion attachment protein receptor (SNARE) proteins at the synapse and to altered exocytosis, suggesting that this may be an early event in the pathogenesis of Parkinson's disease.

Materials and methods

Antibodies

The following antibodies were used: monoclonal anti-α-synuclein syn-1 (BD Transduction, 1:1000); polyclonal anti-α-synuclein PER4 (Spillantini *et al.*, 1998; 1:500); polyclonal phosphorylation-dependent anti-α-synuclein pS129 (Epitomics, 1:500); monoclonal anti-synaptobrevin-2 (Synaptic Systems, 1:1000); monoclonal anti-synaptosomal-associated protein (SNAP)-25 (SMI-81, Sternberger Monoclonals, 1:1000 for immunohistochemistry, 1:10 000 for western blotting; or Abcam, 1:1000); monoclonal anti-syntaxin-1 (HPC-1, Sigma, 1:300 for immunohistochemistry; 1:4000 for western blotting); polyclonal anti-dopamine transporter (Chemicon, 1:1000); polyclonal anti-light-chain-3 (MBL, 1:100); polyclonal anti-β-actin, (Abcam, 1:5000); monoclonal anti-β-actin (Sigma, 1:10 000); monoclonal anti-synphilin (Sigma, 1:1000) and polyclonal anti-glial fibrillary acidic protein (Novus Biological, 1:1000). The following secondary antibodies were used: biotinylated goat anti-rabbit (Vector Laboratories, 1:250) and biotinylated horse anti-mouse (Vector, 1:250). Alexa Fluor-labelled antibodies (Molecular Probes, 1:250) were used for immunofluorescence. Rhodamine-labelled α-bungarotoxin (Molecular Probes) was used at 1 μg/ml.

Transgenic mice

Mice transgenic for human α-syn(1-120) were produced on a C57BL/6S background (Harlan), which lacks mouse α-synuclein (Specht and Schoepfer, 2001; Tofaris *et al.*, 2006). To obtain mice expressing endogenous α-synuclein, α-syn(1-120) mice were crossed with C57BL/6J mice (Charles River), generating line α-syn(1-120E). Homozygosity was determined by quantitative polymerase chain reaction, test breeding and the detection of mouse α-synuclein by immunohistochemistry and immunoblotting. SNAP-25 and syntaxin staining were also performed in 18-month-old human mutant full length A30P α-synuclein mice (Magnani, 2006; Spillantini *et al.*, 2007), 5-month-old human mutant P301S tau transgenic mice (Allen *et al.*, 2002) and 3-month-old R6/2 huntingtin transgenic mice (Mangiarini *et al.*, 1996). Both A30P α-synuclein and P301S tau transgenic mice are on a C57BL/6S background without endogenous mouse α-synuclein, like the (1-120)α-syn transgenic mice. Since A30P α-synuclein and P301S tau transgene expression is driven by the Thy1 promoter and no expression is present in the substantia nigra, the cerebral cortex was used for immunohistochemistry. In R6/2 mice, where the transgene is expressed also in the substantia nigra, the striatum was examined.

Immunohistochemistry

Mice aged 6, 12 or 18 months were deeply anaesthetized and perfused transcardially with 4% paraformaldehyde in 0.1 M phosphate buffer, pH 7.4. Brains were removed and post-fixed overnight, followed by cryoprotection in 30% sucrose in Tris-buffered saline containing 0.02% sodium azide. Serial 30 μm sections were cut on a freezing sledge microtome (Leica). Free-floating sections were quenched in 1.5% hydrogen peroxide, 20% methanol in Tris-buffered saline and blocked in 5% horse serum (monoclonal antibodies) or goat serum (polyclonal antibodies) in Tris-buffered saline with 0.02% Tween for 1 h at room temperature. Sections were incubated with the primary antibody in Tris-buffered saline with 0.02% Tween and, with the exception of anti-α-synuclein antibodies, with 1% horse or goat serum overnight at 4°C. After incubation with biotinylated secondary antibodies (Vector Laboratories), staining was visualized using the ABC Elite Kit (Vector) and 3,3′-diaminobenzidine (Vector Laboratories) as the chromogen. Sections were dehydrated and analysed using a Leitz DMRB microscope. For immunofluorescence, sections were blocked, followed by overnight incubation with primary antibody at 4°C. They were then incubated with the secondary Alexa-labelled antibody. Nuclei were visualized with Hoechst dye (Sigma). Sections were mounted with Permafluor (Thermo) and analyzed with a Leica TCS SPE confocal microscope.

For staining of human sections caudate/putamen and globus pallidus (8 μm), from three controls (average age 69.3 ± 2.18 years) and four patients with Parkinson's disease with non-advanced disease (average age 68.3 ± 6.48 years) were used. Following deparaffinization and antigen retrieval, the sections were incubated with primary antibody overnight at 4°C. They were washed with phosphate buffered saline with 0.02% Tween-20 and incubated with biotinylated goat anti-mouse IgG (1/700) for 2 h at room temperature. This was followed by washes in phosphate buffered saline with 0.02% Tween-20, followed by incubation with avidin-biotin at 1/700 in phosphate buffered saline with 0.02% Tween-20 (Vectastain ABC kit, Vector Laboratories) at room temperature. Following several washes in phosphate buffered saline, the reaction was visualized using 3,3′-diaminobenzidine. Sections were dehydrated, mounted in DPX mounting medium (Lamp Laboratory Supplies) and examined using a Leica Leitz DMRD microscope. Controls for the specificity of the

staining, where the first antibody was omitted, are shown in Supplementary Fig. 3.

α-Bungarotoxin staining

Brain sections were blocked in 0.5% Triton X-100 (Sigma) and 1% bovine serum albumin (Sigma) in phosphate buffered saline and incubated with rhodamine isothiacyanate-labelled α-bungarotoxin (1 μg/ml) at 4°C. Sections were then processed for immunofluorescence.

Extraction of proteasomal subunits and SNARE proteins from mouse brain

Brains were dissected and tissues lysed on ice in 10 vol. or 150 μl of 50 mM Tris-HCl, pH 7.4, 150 mM NaCl, 1% Triton X-100, 0.5% deoxycholic acid (Calbiochem), 0.1% sodium dodecyl sulphate and protease inhibitor cocktail (Roche). Protein concentrations were determined using the BCA Protein Assay Kit (Pierce). Thirty micrograms of protein were run on 10–15% sodium dodecyl sulphate polyacrylamide gel electrophoresis and transferred onto Immobilon P (Millipore). Membranes were blocked in 5% milk Tris-buffered saline with 0.02% Tween and incubated with the primary antibody in 1% milk Tris-buffered saline with 0.02% Tween overnight at 4°C. They were subsequently incubated with horseradish peroxidase-conjugated polyclonal rabbit anti-mouse or polyclonal swine anti-rabbit antibody (DAKO, at 1:5000) in 1% milk Tris-buffered saline with 0.02% Tween. Samples were developed using Western Lightning Chemiluminescence Reagent Plus (Perkin-Elmer). Optical densitometry was performed using NIH Image J software (rsbweb.nih.gov/ij/).

Co-immunoprecipitation

Co-immunoprecipitation was performed as described (McMahon *et al.,* 1995) with minor modifications. Mouse brains or 10^5 PC12 cells were homogenized in 3 ml buffer [0.15 M NaCl, 10 mM HEPES-NaOH, pH 7.4, 1 mM EGTA, 2 mM MgCl₂, protease inhibitor cocktail (Roche)] and solubilized by addition of 1% NP-40. The homogenates were incubated for 30 min on ice and centrifuged for 15 min at 18 000*g*. The resulting supernatants were stored at −20°C until use. 300 μl were pre-cleared by incubation with protein G-Sepharose beads (Amersham) for 1 h at 4°C. Samples were then incubated with either syn-1 antibody or beads (negative control) overnight at 4°C. Next, 50 μl of beads were added to each sample and incubated for 2 h at 4°C. After 6 × 2 min washes with homogenization buffer, 150 μl sodium dodecyl sulphate loading buffer was added to the beads. Samples were run on 12% sodium dodecyl sulphate polyacrylamide gel electrophoresis and immunoblotted. The blots were incubated with antibodies against SNARE proteins overnight at 4°C and for 2 h at room temperature with Protein A/G-horseradish peroxidase antibody (Pierce). Blots were visualized as described above.

Measurement of 26 S proteasome activity

The following reagents were used: fluorogenic substrates Z-Leu-Leu-Glu-AMC (proteasome substrate II, Calbiochem) for caspase-like activity, Suc-Leu-Leu-Val-Tyr-AMC (proteasome substrate III, Calbiochem) for chymotrypsin-like activity, Ac-Arg-Leu-Arg-AMC (Biomol) for trypsin-like activity, epoxomicin (Calbiochem), MG-132 (Biomol), AMC-calibration standard (Biomol), ATP (Sigma), dithiothreitol (Sigma) and digitonin (Merck). Proteasomal acitivity was measured as described (Kisselev and Goldberg, 2005) with minor modifications.

Substantia nigra, olfactory bulb and striatum were dissected, weighed and stored at −80°C. On the day of the assay, samples were homogenized on ice in 10 vol. buffer (50 mM Tris-HCl, pH 7.5, 250 mM sucrose, 5 mM MgCl₂, 2 mM ATP, 1 mM dithiothreitol, 0.5 mM EDTA, 0.025% digitonin) and centrifuged at 18 000*g* for 15 min at 4°C. Supernatants were collected and protein concentrations determined using the BCA-kit (Pierce). For the proteasomal assay, 50 μg protein/sample was used for measurement of chymotrypsin-like and caspase-like activities and 75 μg for trypsin-like activity. Fluorogenic substrates were diluted from stock solutions in proteasome assay buffer (50 mM Tris–HCl, pH 7.5, 40 mM KCl, 5 mM MgCl₂ 0.5 mM ATP, 1 mM dithiothreitol, 0.05 mg/ml bovine serum albumin). Protein samples and fluorogenic substrates were pipetted into a 96-well plate and incubated for 5 min at 37°C. Proteasomal activity was measured at 37°C as an increase in fluorescence over 15 min using a fluorescence plate reader (Ascent Fluroskan FL) with 355 nm excitation/460 nm. Assays were performed in triplicate and proteasome inhibitors epoxomicin (20 μM) and MG-132 (10 μM) were used to demonstrate specificity. A series of dilutions of the AMC standard (16–0.125 μM) was used for calibration.

Aconitase assay

Substantia nigra and striatum from six transgenic and six control mice were dissected on ice, weighed and stored at −80°C. The tissues were homogenized on ice in 10 vol. buffer (320 mM sucrose, 10 mM EDTA, 10 mM Tris-HCl, pH 7.4, 2 mM sodium citrate, 0.6 mM MgCl₂) and diluted 1:20 in the same buffer. The samples were measured in a 96-well plate, as described (Gardner, 2002). Ten microlitres of sample were added to 190 μl of assay buffer (50 mM Tris, 0.4 mM NADP, 5 mM sodium citrate, 0.6 mM MgCl₂, 0.1% Triton, 1 U isocitrate dehydrogenase). The plate was incubated at 37°C and measured in a spectrophotometer (Biotek μQuant) every 4 min for 40 min. Protein concentrations were determined using the BCA-kit (Pierce). The assay was repeated using five wells per sample. Specificity was demonstrated with 200 μM fluorocitrate (a specific inhibitor of aconitase) and the sensitivity with 0.17% hydrogen peroxide.

Isolation of a synaptosome-enriched fraction

The striatum was dissected from transgenic and control mice, rinsed several times in cold buffer (0.32 M sucrose, 1 mM EDTA, 5 mM Tris, 0.25 mM dithiothreitol) and homogenized in 10 vol. of buffer. The extract was then centrifuged for 1 min at 15 000 *g* and the supernatant kept on ice for further use. The Percoll gradients were prepared as described (Dunkley *et al*., 2008) and the tissue homogenates layered on top of the 3% fraction. The tubes were then centrifuged for 5 min at 31 000*g* at 4°C. The synaptosomes were recovered from fractions 2 and 3 at the 10–15% and 15–23% gradient interface. The enriched fractions of striatal synaptosomes were collected, mixed with sample buffer and processed for immunoblotting.

## Vertical microdialysis and dopamine assay

Extracellular dopamine levels were measured in the striatum using vertical microdialysis. Mice were treated with carprofen (0.5 mg/kg i.p.) 30 min prior to probe implantation and anaesthetized with tiletamine-zolazepam (75 mg/kg i.p.) before being placed in a stereotaxic frame. After sagittal cutting, the overlying skin was retracted,

folded away and a hole drilled at the level of the right dorsal striatum (AP = +0.6, L = +1.8, H = −2.1 from the bone); all coordinates (Paxinos, 2001) were taken over the bone and referred to bregma, with bregma and lambda on a horizontal plane. The microdialysis CMA/7 guide cannula (CMA Microdialysis, Stockholm, Sweden) was then gently inserted through the hole using the micromanipulator of the stereotaxic instrument. The cannula was secured with acrylic dental cement and the skin sutured. Mice were housed with free access to food and water to recover from surgery (one mouse per cage). The following day, a CMA/7 microdialysis probe was inserted into the guide cannula and perfused at a constant flow rate (2 μl/min) with artificial cerebrospinal fluid (140 mM NaCl, 7.4 mM glucose, 3 mM KCl, 0.5 mM MgCl$_2$, 1.2 mM CaCl$_2$, 1.2 mM Na2HPO$_4$, 0.3 mM NaH$_2$PO$_4$, pH 7.4). The dialysate was collected at 20 min intervals in tubes containing 5 μl of 10 mM HCl to prevent dopamine oxidation and directly assayed for dopamine, homovanilic acid and 3,4-dihydroxyphenylacetic acid. After a 1 h settling period, five samples were collected to evaluate the baseline release of dopamine and its metabolites. Basal artificial cerebrospinal fluid was then replaced by artificial cerebrospinal fluid containing either 1 μM tetrodotoxin or 50 mM K$^+$ and five more samples were collected to evaluate the response to blockade of voltage-gated Na^{2+} channels or to depolarization. At the end of the experiment, mice were killed by decapitation. Brains were quickly removed and put in 10% formalin, to verify the correct placement of the microdialysis probe. Dopamine, 3,4-dihydroxyphenylacetic acid and homovanillic acid levels in the dialysate were measured by high-performance liquid chromatography. The following mice were used for K$^+$ stimulation: 6-month-old: four controls and five transgenic mice; 12-month-old: six controls and seven transgenic mice; 18-month-old: three controls and three transgenic mice. Differences between transgenic and control mice in dopamine release in the tetrodotoxin and K$^+$ experiments were assessed by two-way ANOVA, followed by Bonferroni's multiple tests for pairwise comparisons. Differences between groups in extracellular 3,4-dihydroxyphenylacetic acid and homovanillic acid levels were assessed by Student's t-test (two-tailed probability). Statistical significance was established at $P < 0.05$. All calculations were performed using GraphPad Prism software version 4.0 (GraphPad, San Diego, CA).

Retention of FM1-43

PC12 cells were transfected with the pIRES2α-syn(1-120), pcDNA3α-syn(1-140) and pcDNA3tau4R constructs using lipofectamine 2000 (Invitrogen). As a control, PC12 cells were transfected with the plasmids without insert. After 48 h, 400 μg/ml G418 (Invitrogen) was added to the growth medium to generate stable cell lines. One million transfected cells were then grown on coverslips in six-well plates. To stimulate synaptic vesicle endocytosis of the FM1-43 dye (Invitrogen), PC12 cells were depolarized with K$^+$ (Hank's balanced salts medium with Ca^{2+} and Mg^{2+} plus 90 mM KCl and 63 mM NaCl). FM1-43 was dissolved in water and diluted in the depolarizing solution. Cells were incubated with 15 μM FM1-43 for 90 s at room temperature. Unbound probe was removed by washing the cells with fresh saline solution for 10 min. To remove background fluorescence, the scavenger dye ADVASEP-7 (SIGMA) was diluted in saline at a concentration of 1 mM and added for 1 min to the culture (Kay et al. 1999). Cells were washed twice with Hanks' balanced salts medium and re-incubated with depolarizing solution for 90 s at room temperature (Gaffield and Betz, 2006). Only vesicles with altered exocytosis were able to retain the dye. The cells were then washed with Hanks' balanced salts medium, fixed with 4% paraformaldehyde and permeabilized with Tris-buffered saline-0.01% Triton X-100 for 12 min at room temperature. Anti α-synuclein antibody (BD Biosciences) was added to the cells and incubated overnight at 4°C. The coverslips were then prepared for microscopic analysis to determine the number of
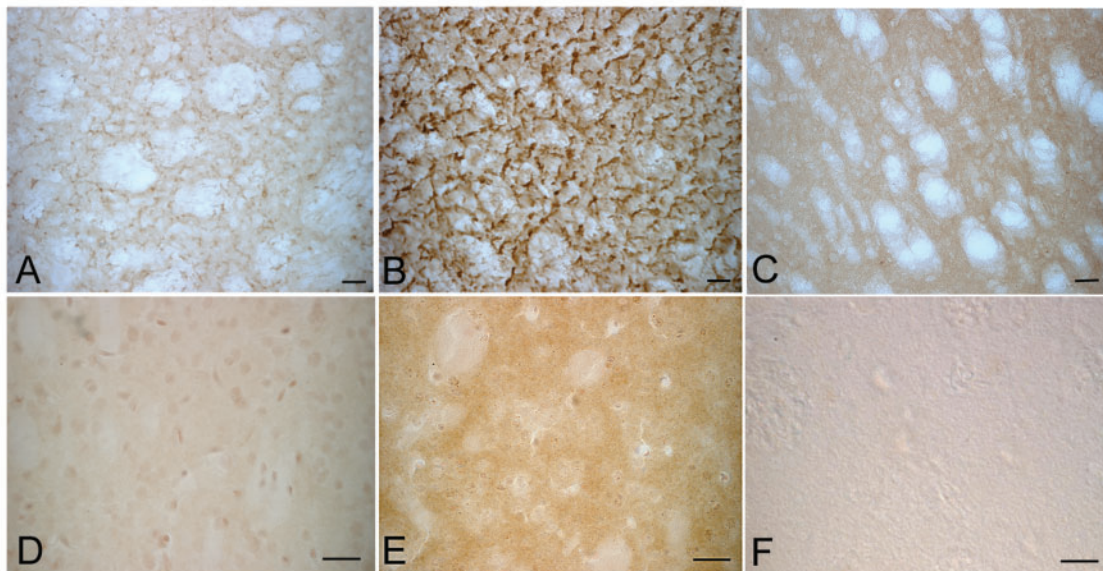
Figure 1 α-Synuclein staining in the striatum of α-syn(1-120) and α-syn(1-120E) transgenic mice. Immunohistochemistry with antibody syn 1, which recognizes both human and mouse α-synuclein, shows clumps of truncated human α-synuclein(1-120) in α-syn(1-120) mice, which lack endogenous α-synuclein (**A**). α-Syn(1-120E) mice, which express human α-synuclein(1-120) in the presence of endogenous mouse α-synuclein, also show marked accumulation of α-synuclein (**B**) compared to the rather homogeneous α-synuclein staining in C57BL/6J control mice (**C**). An antibody specific for α-synuclein phosphorylated at Ser129 (PSer129) shows staining in α-syn(1-120E) mice (**E**) but not in α-syn(1-120) (**D**) or C57BL/6J control mice (**F**). Scale bar = 20 μm.
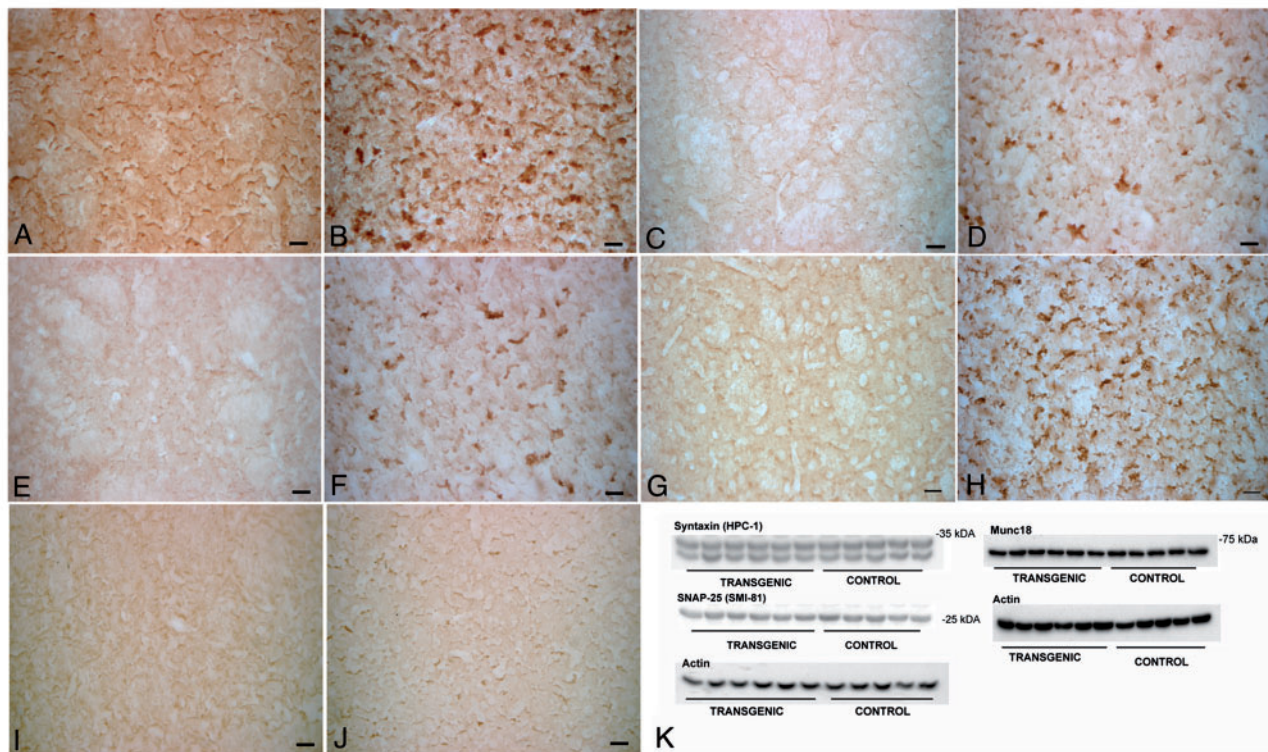
Figure 2 Accumulation of SNARE proteins in the striatum of α-syn(1-120) mice. Immunohistochemistry for SNARE proteins in the striatum of 18-month-old α-syn(1-120) mice and control mice shows accumulation of SNAP-25 (**B**), syntaxin-1 (**D**) and synaptobrevin-2 (**F**) in transgenic but not in control mice (**A, C, E**). α-Syn(1-120E) mice also show accumulation of SNAP-25 (**H**) unlike C57BL/6J mice (**G**). The difference in SNAP-25 staining between 6-month-old α-syn(1-120) mice (**J**) and C57BL/6S controls (**I**) is much less pronounced. No significant differences were present in the expression of SNARE proteins between transgenic mice and controls (**K**). Scale bars = 20 μm.

cells that retained FM1-43. The signal could be detected using a typical fluorescein emission channel (488 channel in a Leica CTR 6000 fluorescence microscope).

A total of 1000–1500 cells (identified by 4′,6-diamidino-2-phenylin-dole nuclear staining) was counted per coverslip. Two coverslips were counted for each experimental condition and each experiment was repeated at least three times. Only cells with fluorescent granular staining indicative of vesicular retention of dye were counted for the controls; for transfected cells expressing human proteins, α-synuclein-and tau-positive cells that were also positive for FM1-43 were counted. Statistical analysis was performed using *t*-test in Prism 3.0 software (La Jolla, CA, USA).

Results

Accumulation of α-synuclein in pre-synaptic nerve terminals

We hypothesized that in α-syn(1-120) mice dopaminergic dys-function may result from an effect of α-synuclein at its normal location at the pre-synaptic terminal. We therefore examined the distribution of human α-synuclein(1-120) in the striatum from transgenic mice without endogenous α-synuclein and in control mice with and without endogenous α-synuclein. Using antibody syn-1, which recognizes both human and mouse α-synuclein, we observed synaptic accumulation of truncated human α-synuclein in

transgenic (Fig. 1A), but not in control mice (Fig. 1C). In order to determine whether the presence of endogenous α-synuclein can affect this pattern, the α-syn(1-120) mice were crossed with C57BL/6J mice to generate the α-syn(1-120E) line. Immunohistochemistry showed that α-synuclein aggregates were abundant in the striatum (Fig. 1B). We next investigated whether endogenous α-synuclein was present in the inclusions in α-syn(1-120E) mice. Antibodies directed against the C-terminus of α-synuclein (data not shown) or specific for α-synuclein phosphory-lated at Ser129 (PSer129) (Fujiwara *et al.*, 2002)–two epitopes not present in the transgenic protein–labelled some aggregates in α-synuclein(1-120E) mice (Fig. 1E), indicating the presence of en-dogenous mouse protein in the aggregates. No staining for PSer129 was found in α-syn(1-120) mice (Fig. 1D) or in control mice with (Fig. 1F) or without (data not shown) endogenous α-synuclein. The specificity of the anti-α-synuclein pS129 antibody was tested by immunoblotting of α-syn(1-120E) brain extracts before and after alkaline phosphatase treatment (Supplementary Fig. 2A).

Age-dependent redistribution of SNARE proteins in dopaminergic terminals of transgenic mice

Recent work has suggested a role for α-synuclein in SNARE-mediated exocytosis at the synapse (Chandra *et al.*, 2005;
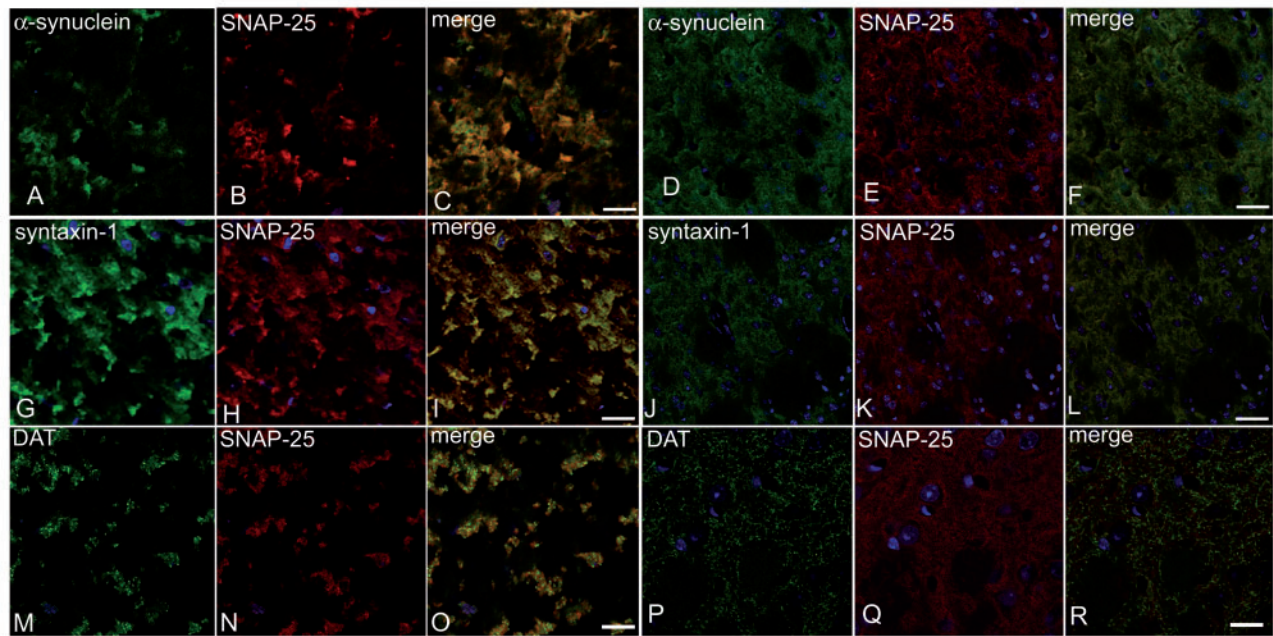
Figure 3 α-Synuclein and SNARE proteins co-localize in the striatum of α-syn(1-120) mice. Confocal imaging shows that aggregates containing truncated α-synuclein (**A**) and SNAP-25 (**B**) co-localize (**C**). The distribution of mouse α-synuclein (**D**) and SNAP-25 (**E**) is homogeneous (**F**) in control mice. Confocal imaging shows co-localization (**I**) of accumulated syntaxin-1 (**G**) and SNAP-25 (**H**). Note the homogeneous distribution of syntaxin-1 (**J**) and SNAP-25 (**K**) in control mice. Dopamine transporter (DAT) (**M**) and SNAP-25 (**N**) co-localize (**O**). Dopamine transporter and SNAP-25 staining differs between transgenic and C57BL/6S control mice (**P–R**). Bar = 20 μm (**A–F**), 10 μm (**G–L**).

Larsen et al., 2006). We therefore investigated the localization of SNAP-25, syntaxin-1 and synaptobrevin-2 in the striatum of α-syn(1-120) mice. In contrast to control mice, where staining was homogenous (Fig. 2A, C, E and G), a marked redistribution of SNARE proteins was observed in the striatum of α-syn(1-120) (Fig. 2B, D and F) and α-syn(1-120E) (Fig. 2H) mice. It was further investigated in α-syn(1-120) mice, where this effect was age-dependent, being very low at 6 months (Fig. 2I–J, Supplementary Fig. 1), intermediate at 12 months (Supplementary Fig. 1) and maximal at 18 months (Fig. 2B, D and F). By immunoblotting, the levels of syntaxin-1, SNAP-25 and Munc-18 were unchanged in the striatum of 6 and 18-month-old transgenic mice, indicating that compared to age-matched controls, SNARE proteins were redistributed, but not overexpressed (Fig. 2K, Supplementary Fig. 2G). In α-syn(1-120) mice, clusters of truncated α-synuclein and SNAP-25 co-localized in striatal nerve terminals (Fig. 3A–C). In contrast, control mice showed a homogeneous distribution of α-synuclein and SNAP-25 (Fig. 3D–F). Confocal imaging of sections from α-syn(1-120) mice that were double stained for SNAP-25 and syntaxin-1 (Fig. 3G–I) demonstrated that SNARE proteins co-localized in the synaptic terminal aggregates. Moreover, we confirmed that accumulation of SNARE proteins was present in dopaminergic nerve terminals by double staining of striatal sections with antibodies against SNAP-25 and the plasma membrane dopamine transporter (Fig. 3M–R). The staining pattern of dopamine transporter differed between control and transgenic mice (Fig. 3M–R). In the transgenic mice, it only partially overlapped with the staining for SNARE

proteins. Double labelling using SNAP-25 antibodies, in conjunction with α-bungarotoxin, synaptobrevin-2 antibodies or synaptophysin antibodies, confirmed that SNARE proteins accumulated in synaptic nerve terminals (Fig. 4). No direct interaction between full-length or truncated α-synuclein and SNAREs was detected by immunoprecipitation (Supplementary Fig. 2C and D) although in control experiments the anti-syntaxin-1 antibody precipitated synaptobrevin-2 in brain extract (Supplementary Fig. 2D) and the anti-synphilin antibody precipitated α-synuclein in PC12 cell extract (Supplementary Fig. 2E). The synaptic localization of α-syn(1-120) and SNARE proteins was also confirmed by immunoblotting of synaptosomal preparations with anti-α-synuclein and anti-syntaxin-1 antibodies (Supplementary Fig. 2B).

Unaltered proteasomal function and subunit composition, aconitase activity and levels of autophagy in α-syn(1-120) mice

Altered degradation of α-synuclein and increased oxidative stress have been considered possible factors causing α-synuclein dysfunction in Parkinson's disease. Using an in vitro assay, we detected no significant differences in the three major proteasomal activities (trypsin-like, chymotrypsin-like and capase-like) between transgenic and control mice at 18 months of age (Fig. 5A). Immunoblots of nigral extracts of 18-month-old mice did not reveal any changes in proteasomal subunit composition between
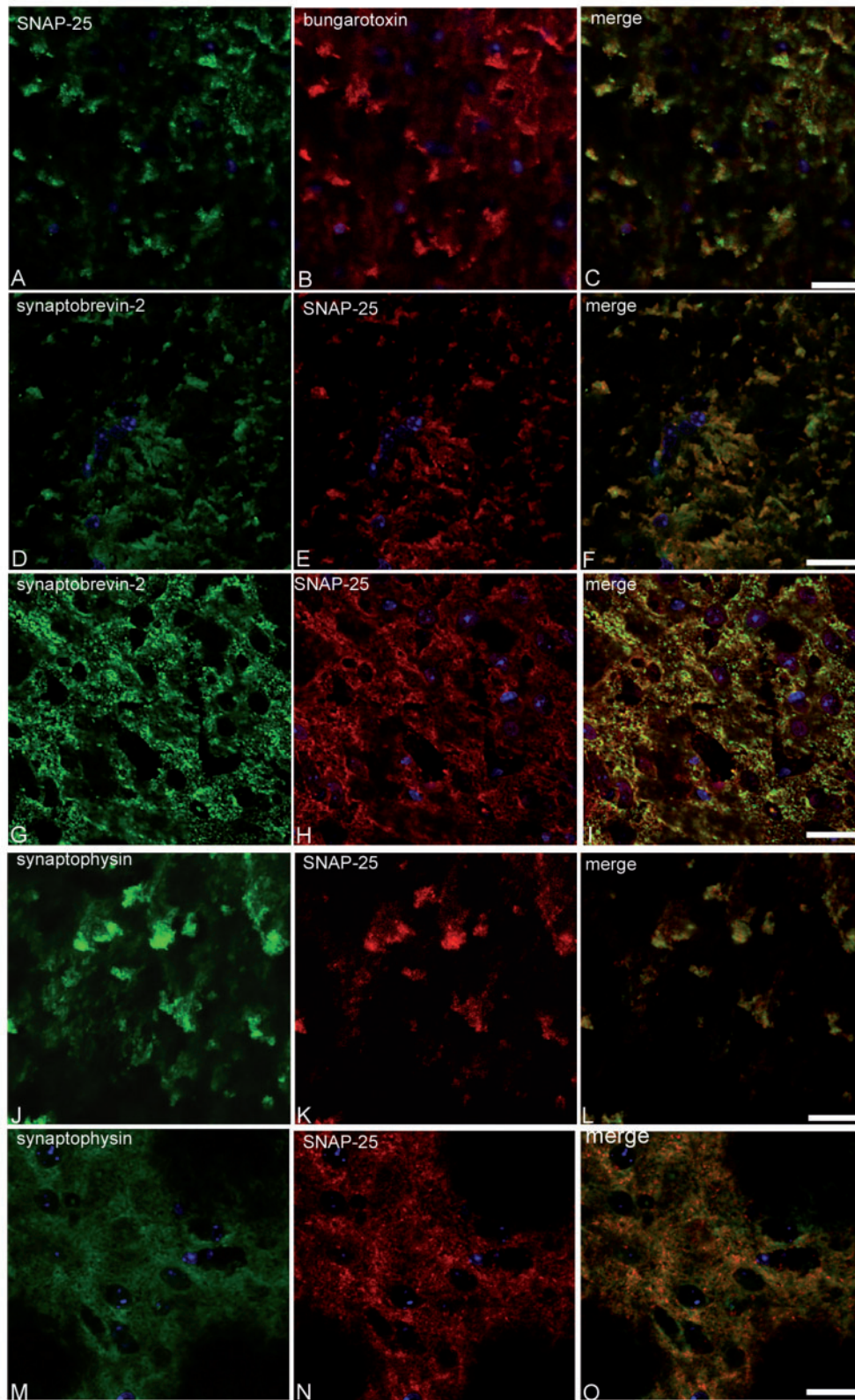
Figure 4 Redistribution of SNARE proteins in the striatum of α-syn(1-120) transgenic mice. Co-localization (**C**) of SNAP-25 (**A**) and α-bungarotoxin (**B**). Synaptobrevin-2 (**D**) and SNAP-25 (**E**) also co-localize (**F**). The same is true (**L**) of synaptophysin (**J**) and SNAP-25 (**K**). In control mice, synaptobrevin-2 and SNAP-25 staining (**G–I**) and synaptophysin and SNAP-25 staining (**M–O**) are homogeneous. Scale bars = 25 μm (**A–C**), 20 μm (**D–I**), 15 μm (**J–O**).
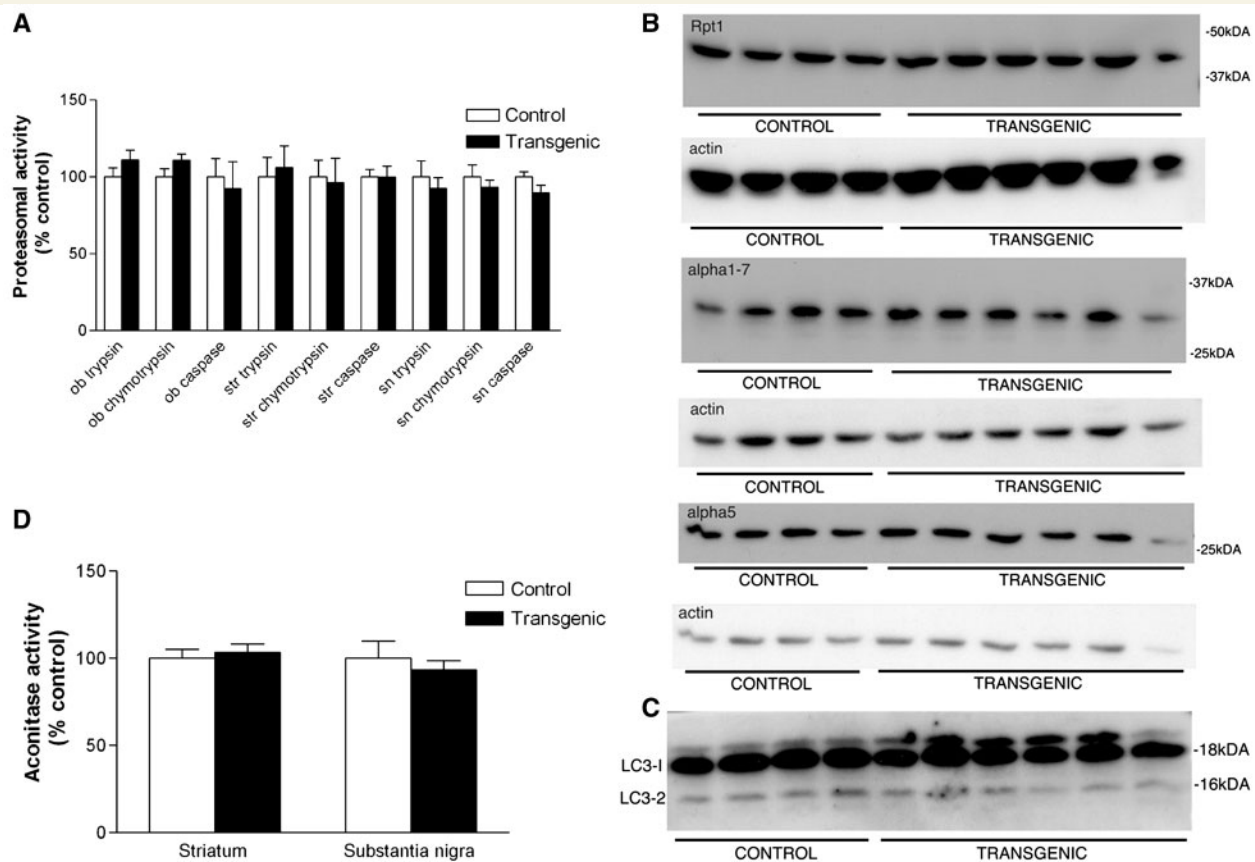
Figure 5 No change in the ubiquitin-proteasome system, autophagy or oxidative stress in α-syn(1-120) transgenic mice. Proteasomal activities in the striatum of α-syn(1-120) mice at 18 months of age. Trypsin-, chymotrypsin- and caspase-like activities did not differ between transgenic and control mice (**A**). Immunoblots of nigral extracts from 18-month-old control ($n = 4$) and α-syn(1-120) ($n = 6$) mice showed no changes in the levels of proteasomal subunits Rpt1, alpha 1.7 or alpha 5 (**B**). Immunoblot of nigral extracts from 18-month-old control ($n = 4$) and α-syn(1-120) ($n = 6$) mice showed no change in the level of the autophagosomal marker LC3-2 (**C**). Aconitase activity in striatum and substantia nigra of 18-month-old α-syn(1-120) mice did not differ from that of control mice (**D**).

the two groups (Fig. 5B). Western blot analysis of the autophagosomal protein light-chain-3 (LC3-2) showed no change in transgenic mice (Fig. 5C). Mitochondrial dysfunction accompanied by an increase in oxidative stress is thought to play a role in the pathogenesis of Parkinson's disease (Zhou *et al.*, 2008). To look for an increase in oxidative stress in α-syn(1-120) mice, we used an enzymatic assay that measures the activity of the oxidative stress-sensitive citric acid cycle enzyme aconitase (Gardner, 2002). We did not find any change in aconitase activity in the substantia nigra or striatum of transgenic mice compared to controls (Fig. 5). However, further work is required to definitively rule out an increase in oxidative stress.

## SNARE protein redistribution is specific to α-synuclein aggregation

We next investigated whether the accumulation of SNARE proteins was specific to the expression of truncated α-synuclein. We examined the distribution of SNAP-25 and syntaxin-1 in a mouse line expressing full-length human mutant A30P α-synuclein under the control of the murine Thy 1.2 promoter on a mouse α-synuclein null

background (Magnani, 2006; Spillantini *et al.*, 2007). Accumulation of SNARE proteins was also seen in this line (Fig. 6A and B), but not in the cerebral cortex of control mice (Supplementary Fig. 3D). To determine whether accumulation of SNARE proteins is characteristic of other models of human neurodegenerative disease, we stained brain sections from human mutant P301S tau mice, a model of tauopathy (Allen *et al.*, 2002) and from R6/2 mice, a model of Huntington's disease (Mangiarini *et al.*, 1996). Although we observed some changes in SNAP-25 staining between control mice and mice transgenic for human P301S tau, the pattern was distinct from that in α-syn(1-120) and A30P mice (Fig. 6C). We failed to observe significant changes in syntaxin-1 staining in P301S tau mice (Fig. 6D). No accumulation of SNAP-25 or syntaxin-1 was seen in the striatum of R6/2 mice (Fig. 6E and F).

SNARE protein redistribution is a feature of Parkinson's disease

To investigate whether SNARE proteins accumulate in Parkinson's disease, we stained brain sections from three cases of idiopathic Parkinson's disease and one case of familial Parkinson's disease
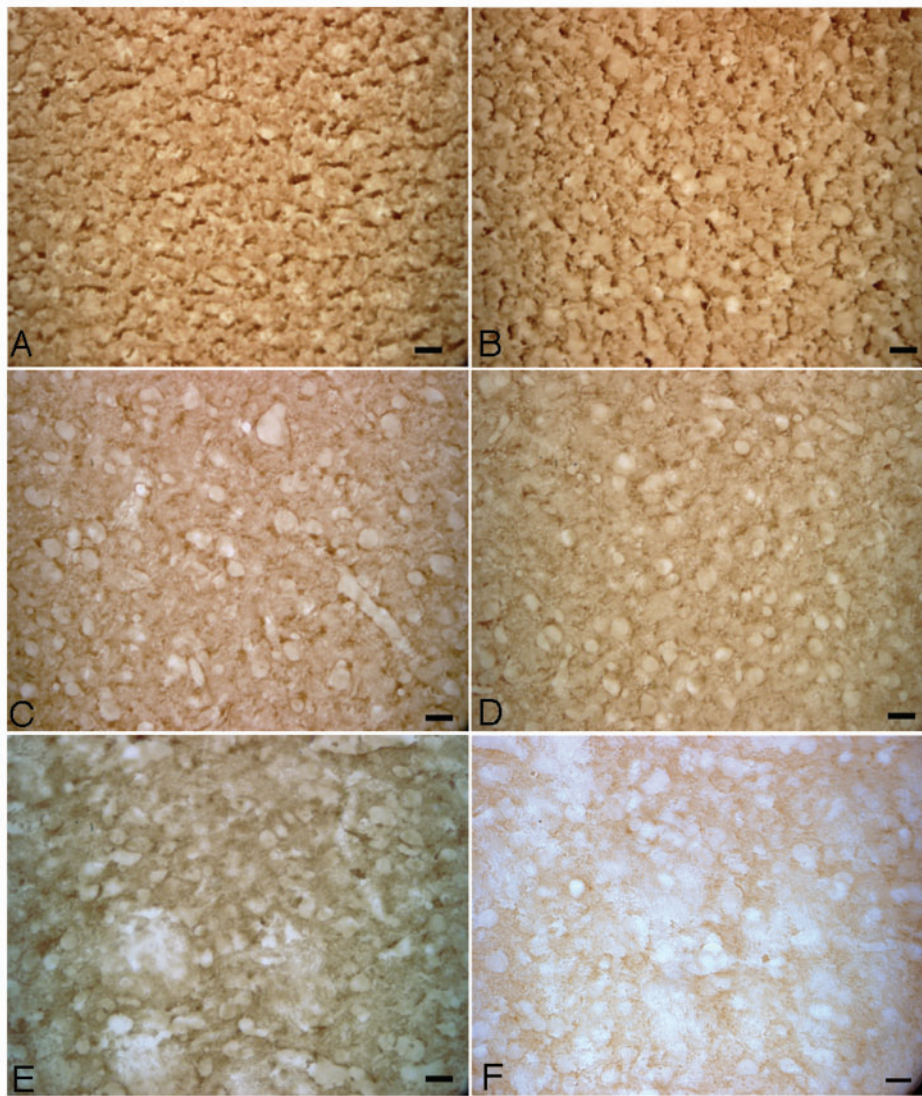
Figure 6 SNARE protein staining in transgenic mouse models of human neurodegenerative diseases. Staining of cerebral cortex from mice transgenic for human mutant A30P α-synuclein for SNAP-25 (**A**) and syntaxin-1 (**B**) shows a similar accumulation of SNARE proteins as in mice transgenic for α-syn(1-120). Staining of cerebral cortex from mice transgenic for human mutant P301S tau for SNAP-25 (**C**) and syntaxin-1 (**D**) shows a pattern distinct from that of the mouse lines transgenic for α-synuclein. No accumulation of SNAP-25 (**E**) or syntaxin-1 (**F**) was observed in the striatum from transgenic mice expressing human mutant huntingtin (line R6/2). Scale bars = 20 μm.

with the A53T mutation in α-synuclein (Fig. 7). Strikingly, SNAP-25, syntaxin-1 and α-synuclein accumulated in the striatum of Parkinson's disease cases (Fig. 7B, D and F), when compared with age-matched controls (Fig. 7A, C and E), indicating that our observations in transgenic mice are of significance for the human disease.

Pre-synaptic accumulation of α-synuclein and redistribution of SNARE proteins are associated with reduced dopamine release

We monitored the release of dopamine by microdialysis to investigate whether the accumulation of α-synuclein and SNARE proteins was associated with synaptic failure (Fig. 8). Dopamine levels were significantly reduced in α-syn(1-120) transgenic mice (-43%, $P<0.01$, data not shown), in accordance with our previous findings (Tofaris *et al.*, 2006). Microdialysis in the striatum of 12-month-old transgenic mice showed that perfusion of the dialysis probe with Ringer solution containing 1 μM tetrodotoxin resulted in a significant decrease in dopamine release in both transgenic (-49%, $P<0.01$) and control (-78%, $P<0.01$) mice (Supplementary Fig. 4A), confirming the neuronal origin of released dopamine. We then monitored dopamine levels by microdialysis to investigate whether the accumulation of α-synuclein and SNARE proteins was associated with synaptic failure (Fig. 8A–F).

Basal and K$^+$-stimulated levels of released dopamine were similar in the striatum of 6-month-old α-syn(1-120) mice and control
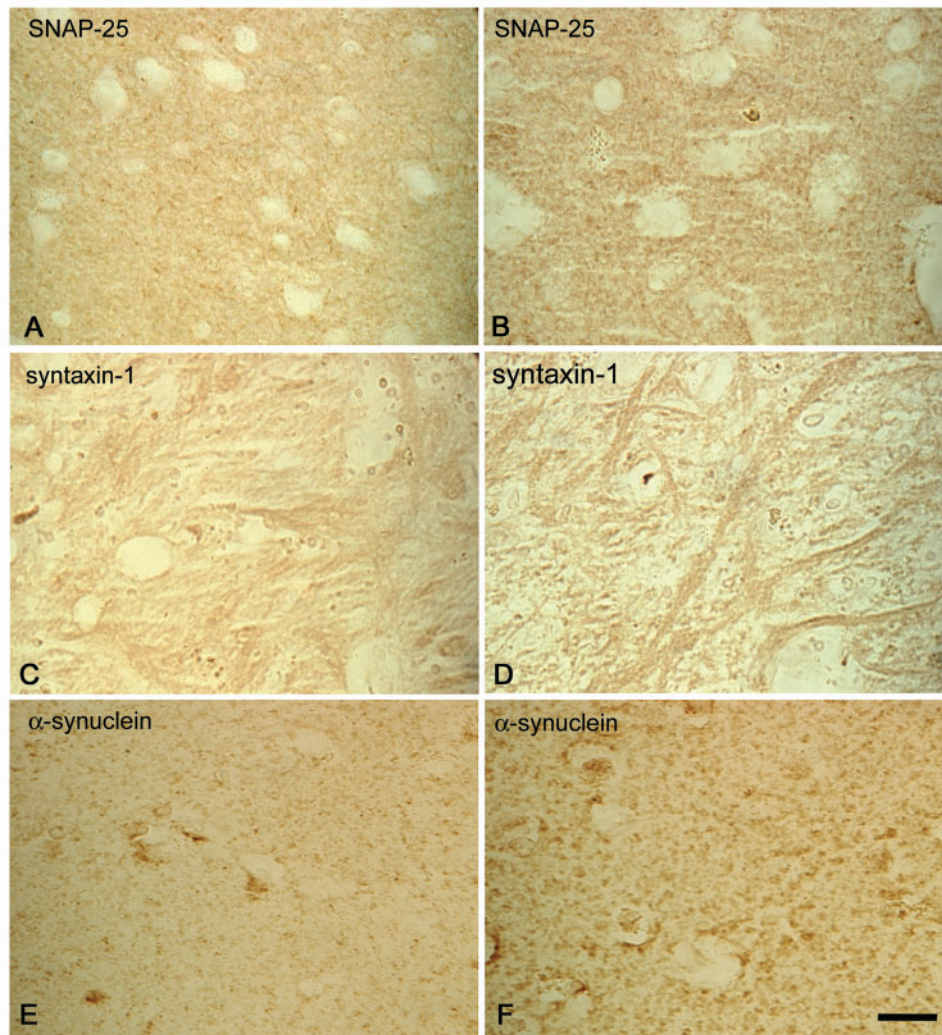
Figure 7 Redistribution of SNARE proteins in Parkinson's disease. Immunohistochemistry for SNAP-25 (**A**, **B**), syntaxin-1 (**C**, **D**) and α-synuclein (**E**, **F**) in the striatum (putamen **A**, **B**, **E**, **F**; external globus pallidus **C**, **D**) of control (**A**, **C**, **E**) and Parkinson's disease (**B**, **D**, **F**) brains. Images are representative of $n = 3$ for control brains and $n = 4$ for Parkinson's disease brains. Scale bar = 5 µm.

mice (Fig. 8A). K$^+$ stimulation significantly increased dopamine release in transgenic (* + 145%, $P < 0.001$) and control (* + 184%, $P < 0.001$) mice (Fig. 8A and D), where * indicates comparison between values before and after K$^+$, and ° indicates comparison between wild type and transgenic mice basal levels. At 12 months of age, control and α-syn(1-120) transgenic mice responded differently to depolarization (Fig. 8B). Basal dopamine levels were significantly lower (°- 48%, $P < 0.001$) in α-syn(1-120) mice when compared to controls (Fig. 8E). Furthermore, while striatal synapses of control mice responded to depolarisation by 50 mM K$^+$ with an increase in dopamine release of 199% (Fig. 8D, $P < 0.001$), evoked dopamine release from striatal synapses of transgenic α-syn(1-120) mice was not significantly different from basal levels. Dopaminergic synaptic dysfunction was still present in 18-month-old α-syn(1-120) mice (Fig. 8C). Basal levels of dopamine were lower in transgenic mice compared to controls (−73.55%, $P < 0.001$, Fig. 8F). This reduction was more pronounced than at 12 months. Potassium-evoked depolarization resulted in significant dopamine release in control mice

(*+ 132.6%; $P < 0.001$), but not in transgenic mice (Fig. 8F), indicating progressive synaptic failure in association with an increase in SNARE redistribution. We also measured the levels of the dopamine metabolites 3,4-dihydroxyphenylacetic acid and homovanillic acid (Supplementary Fig. 4) at 6, 12 and 18 months and detected a progressive reduction in the α-syn(1-120) transgenic mice when compared to controls, in agreement with the reduction in released dopamine.

α-Synuclein expression alters exocytosis of FM1-43 in PC12 cells

To examine whether the accumulation of α-synuclein interferes with exocytosis, we studied the release of FM1-43 from PC12 cells that stably expressed human α-syn(1-120) (Gaffield and Betz, 2006). Potassium-evoked release was significantly reduced compared to that from cells transfected with empty vector
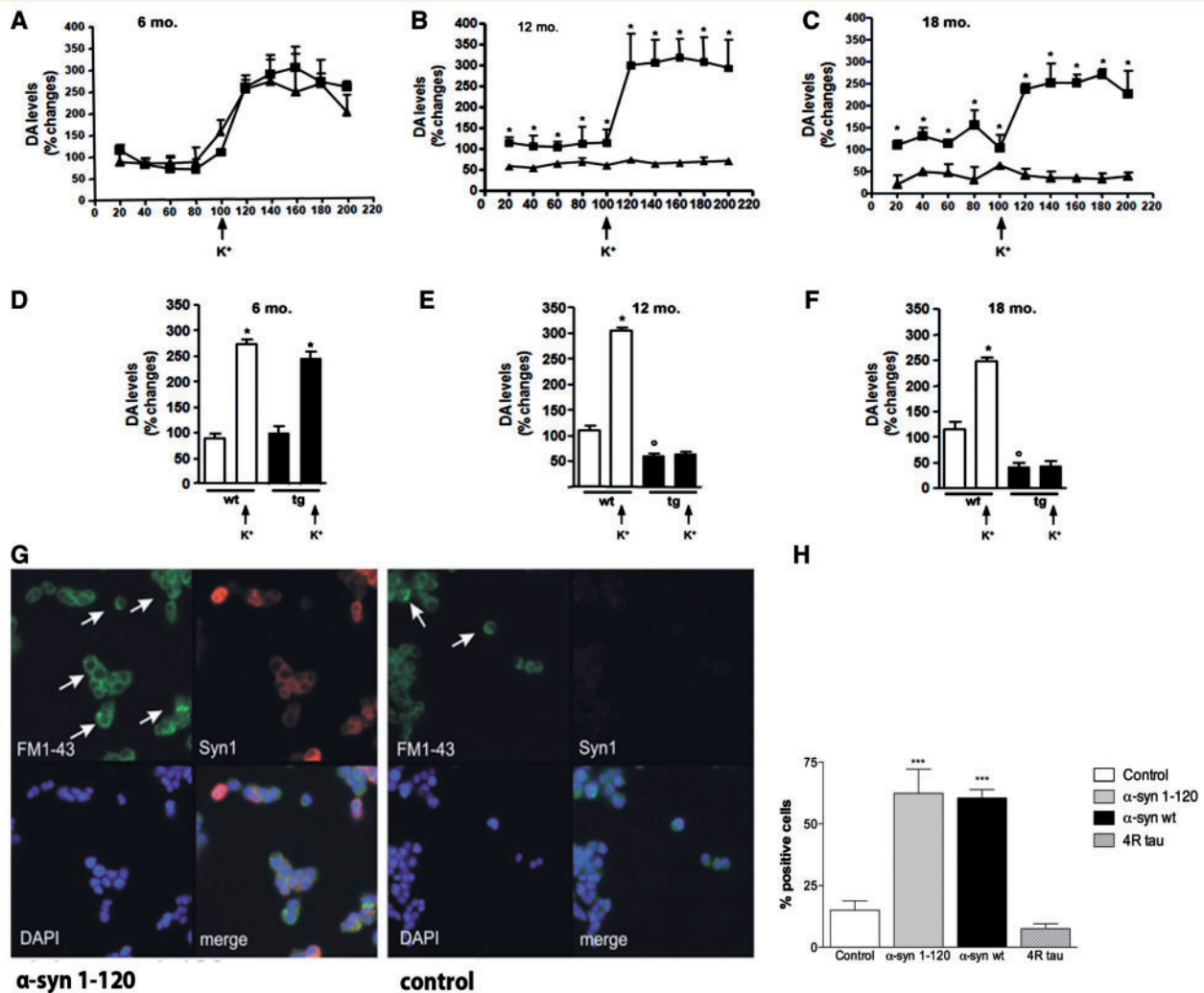
Figure 8 Reduction in dopamine release in the striatum of α-syn(1-120) mice (**A–F**) and impairment in exocytosis in PC12 cells expressing human α-synuclein (**G**, **H**). Dopamine (DA) levels change during collection of dialysate from the striatum of 6- (**A**), 12- (**B**) and 18- (**C**) month-old α-syn(1-120) (filled diamond) and C57/BL6S control (filled squares) mice. During microdialysis two collecting periods were selected: 100 min of basal sample collection and 100 min of perfusion with artificial cerebrospinal fluid containing 50 mM K$^+$. At 12 and 18 months of age, both basal and K$^+$-evoked dopamine release were significantly lower in the α-syn(1-120) mice than in age-matched controls. No differences were present in 6-month-old mice. Mean basal and K$^+$-evoked dopamine levels in 6- (**D**), 12- (**E**) and 18- (**F**) month-old wild-type (wt; white bars) and α-syn(1-120) transgenic (tg; black bars) mice. Potassium stimulation (K$^+$) significantly increased dopamine release in both 6-month-old controls and α-syn(1-120) transgenic mice (**D**). Potassium induced a statistically significant increase in dopamine release in 12-month-old controls but not in 12-month-old α-syn(1-120) transgenic mice (**E**). The same was true when 18-month-old α-syn(1-120) mice were compared to age-matched controls (**F**). (*$P<0.001$ value before and after K$^+$ stimulation; °$P<0.001$ between wild-type and transgenic basal levels). PC12 cells expressing human α-synuclein(1-120) retained significantly more FM1-43 dye (bright green) than cells transfected with empty vector (**G**). Only cells with dot-like bright green fluorescence (arrows) were counted. PC12 cells expressing full-length human α-synuclein retained more FM1-43 dye than cells transfected with empty vector or PC12 cells expressing 4R0N tau (**H**). Statistical analysis was performed using Student's *t*-test, ***$P<0.005$. Data represent the mean of three independent experiments. In each experiment two coverslips were counted for each condition, with 1000–1500 cells per coverslip.

(Fig. 8G and H). Similar results were obtained in PC12 cells stably expressing full-length human α-synuclein (Fig. 8H). By contrast, FM1-43 release was not impaired in PC12 cells stably expressing the 383 amino acid isoform of human brain tau (Fig. 8H). Extraction of α-synuclein from PC12 cells and staining with thioflavin S did not show any filaments (data not shown), although we cannot exclude the presence of low levels of oligomeric α-synuclein. High-molecular weight bands, possibly corresponding

to oligomeric α-synuclein, were present in α-syn(1-120) transgenic mouse brain lysates (Supplementary Fig. 2F).

Discussion

The study of the striatum of α-syn(1-120) transgenic mice has shown that expression of truncated and full-length human

α-synuclein leads to a redistribution of SNARE proteins, with an associated reduction in exocytosis and dopamine release. Furthermore, antibodies recognising epitopes in the last 20 amino acids of α-synuclein stained some aggregates in α-syn(1-120E) mice, which express mouse α-synuclein in addition to truncated human α-synuclein. This indicates that the full-length mouse protein can be recruited to aggregates made of truncated human protein.

It has been suggested that the aggregation of α-synuclein in nerve terminals causes synaptic dysfunction in Parkinson's disease and dementia with Lewy bodies (Kramer and Schulz-Schaeffer, 2007). Furthermore, dopamine deficiency occurs early in the course of Parkinson's disease, where it is believed to precede nerve cell death (Hornykiewicz, 1998). Similarly, accumulation of α-synuclein in nerve terminals has been shown to precede nerve cell death in sympathetic ganglia in Parkinson's disease (Orimo et al., 2008). It follows that the mouse line transgenic for human α-syn(1-120) may model the early stages of Lewy body disease. The accumulation of α-synuclein and SNAREs at synaptic nerve terminals in transgenic mice and in Parkinson's disease, in conjunction with impaired dopamine release in both transgenic mouse brain and transfected PC12 cells, points to a gain of toxic function of α-synuclein at the synapse. This is consistent with previous findings in transfected cells showing that overexpression of α-synuclein inhibits evoked neurotransmitter release by acting at a step between vesicle docking and fusion (Larsen et al., 2006). Interestingly, this process does not appear to be affected by the last 20 amino acids of α-synuclein, in that it was present in PC12 cells overexpressing either full-length α-synuclein or α-syn(1-120), as well as in transgenic mice expressing mutant full-length human A30P α-synuclein.

Synaptic dysfunction has also been implicated in the pathogenesis of Alzheimer's disease (Selkoe, 2002; Arendt, 2009). In the present study, we failed to observe an overall redistribution of SNARE proteins in transgenic mouse models of tauopathy and Huntington's disease, suggesting that early synaptic failure due to SNARE redistribution is limited to some neurodegenerative diseases and is not a general feature of protein aggregation diseases. It remains to be determined how α-synuclein can lead to a redistribution of SNAREs. It could be that a balance between monomeric α-synuclein and SNARE proteins is necessary for proper SNARE assembly and function; alternatively, it could be that an increase in α-synuclein causes the formation of toxic oligomers that affect SNARE distribution and function. In both cases the final result would be impaired exocytosis.

In agreement with previous findings we failed to detect a direct interaction between SNARE proteins and α-synuclein (Chandra et al., 2005; Larsen et al., 2006). Similarly, the mechanisms underlying the redistribution of dopamine transporter remain to be identified. Previous work has shown that α-synuclein can influence dopamine transporter function (Sidhu et al., 2004; Bellucci et al., 2008). This is supported by the finding that mouse neurons and human neuroblastoma cells lacking α-synuclein are resistant to the mitochondrial complex 1 inhibitor 1-methyl-4-phenyl-1,2,3,6-tetrahydropyridine (MPTP) (Dauer et al., 2002; Fountaine et al., 2008).

In a recent rat model of α-synucleinopathy produced by injection of recombinant adeno-associated virus 2 expressing human mutant A53T α-synuclein under the control of a neuron-specific synapsin promoter, changes in the levels of synaptic, cytoskeletal and motor proteins were observed (Chung et al., 2009). In agreement with this study, we also found signs of neuroinflammation in the α-syn(1-120) mice (Tofaris et al., 2006). However, we failed to observe changes in the levels of SNARE proteins in our mice.

Taken together, the present findings indicate that, as a result of the accumulation of α-synuclein, Parkinson's disease may be characterized by a dying-back mechanism that begins at the synapse and leads to axonal degeneration in the striatum, followed by the degeneration of dopaminergic nerve cells in the substantia nigra. These findings are in agreement with the hypothesis that it is the process leading to the formation of Lewy bodies and Lewy neurites that causes neurodegeneration (Orimo et al., 2008; Greffard et al., 2010). Inhibition of α-synuclein toxicity at the synapse could be an effective treatment for Parkinson's disease.

Acknowledgements

Funding

Supplementary material

Supplementary material is available at *Brain* online.

References

Allen B, Ingram E, Takao M, Smith MJ, Jakes R, Virdee K, et al. Abundant tau filaments and nonapoptotic neurodegeneration in transgenic mice expressing human P301S tau protein. J Neurosci 2002; 22: 9340–51.

Arendt T. Synaptic degeneration in Alzheimer's disease. Acta Neuropathol 2009; 118: 167–79.

Baba M, Nakajo S, Tu PH, Tomita T, Nakaya K, Lee VM, et al. Aggregation of α-synuclein in Lewy bodies of sporadic Parkinson's disease and dementia with Lewy bodies. Am J Pathol 1998; 152: 879–84.

Bellucci A, Collo G, Sarnico I, Battistin L, Missale C, Spano P. Alpha-synuclein aggregation and cell death triggered by energy deprivation

and dopamine overload are counteracted by D2/D3 receptor activation. J Neurochem 2008; 106: 560–77.

Chandra S, Gallardo G, Fernandez-Chacon R, Schlüter OM, Südhof TC. Alpha-synuclein cooperates with CSPα in preventing neurodegeneration. Cell 2005; 123: 383–96.

Chung CY, Koprich JB, Siddiqi H, Isacson O. Dynamic changes in presynaptic and axonal transport proteins combined with striatal neuroinflammation precede dopaminergic neuronal loss in a rat model of AAV α-synucleinopathy. J Neurosci 2009; 29: 3365–73.

Crowther RA, Jakes R, Spillantini MG, Goedert M. Synthetic filaments assembled from C-terminally truncated α-synuclein. FEBS Lett 1998; 436: 309–12.

Dauer W, Kholodilov N, Vila M, Trillat AC, Goodchild R, Larsen KE, et al. Resistance of α-synuclein null mice to the parkinsonian neurotoxin MPTP. Proc Natl Acad Sci USA 2002; 99: 14524–9.

Dunkley PR, Jarvie PE, Robinson PJ. A rapid Percoll gradient procedure for preparation of synaptosomes. Nat Protoc 2008; 3: 1718–28.

Fountaine TM, Venda LL, Warrick N, Christian HC, Brundin P, Channon KM, et al. The effect of α-synuclein knockdown on MPP+ toxicity in models of human neurons. Eur J Neurosci 2008; 28: 2459–73.

Fujiwara H, Hasegawa M, Dohmae N, Kawashima A, Masliah E, Goldberg MS, et al. α-Synuclein is phosphorylated in synucleinopathy lesions. Nat Cell Biol 2002; 4: 160–4.

Gaffield MA, Betz WJ. Imaging synaptic vesicle exocytosis and endocytosis with FM dyes. Nat Protoc 2006; 1: 2916–21.

Gardner PR. Aconitase: sensitive target and measure of superoxide. Methods Enzymol 2002; 349: 9–23.

Goedert M. Alpha-synuclein and neurodegenerative diseases. Nat Rev Neurosci 2001; 2: 492–501.

Greffard S, Verny M, Bonnet AM, Seilhear D, Hauw JJ, Duyckaerts C. A stable proportion of Lewy body-bearing neurons in the substantia nigra suggests a model in which the Lewy body causes neuronal death. Neurobiol Aging 2010; 31: 99–103.

Hornykiewicz O. Biochemical aspects of Parkinson's disease. Neurology 1998; 51: S2–9.

Ibanez P, Bonnet AM, Débarges B, Lohmann E, Tison F, Pollak P, et al. Causal relation between alpha-synuclein gene duplication and familial Parkinson's disease. Lancet 2004; 364: 1169–71.

Kay AR, Alfonso A, Alford S, Cline HT, Holgado AM, Sakmann B, et al. Imaging synaptic activity in intact brain and slices with FM1-43 in *C. elegans*, lamprey and rat. Neuron 1999; 24: 809–17.

Kisselev AF, Goldberg AL. Monitoring activity and inhibition of 26S proteasome with fluorogenic peptide substrate. Methods Enzymol 2005; 398: 364–78.

Kramer ML, Schulz-Schaeffer WJ. Presynaptic alpha-synuclein aggregates, not Lewy bodies, cause neurodegeneration in dementia with Lewy bodies. J Neurosci 2007; 27: 1405–10.

Krüger R, Kuhn W, Müller T, Woitalla D, Graeber M, Kösel S, et al. Ala30Pro mutation in the gene encoding α-synuclein in Parkinson's disease. Nature Genet 1998; 18: 106–8.

Larsen KE, Schmitz Y, Troyer MD, Mosharov E, Dietrich P, Quazi AZ, et al. α-Synuclein overexpression in PC12 and chromaffin cells impairs catecholamine release by interfering with a late step in exocytosis. J Neurosci 2006; 26: 11915–22.

Liu CW, Giasson BI, Lewis KA, Lee VM, DeMartino GN, Thomas PJ. A precipitating role for truncated α-synuclein and the proteasome in α-synuclein aggregation: implications for pathogenesis of Parkinson disease. J Biol Chem 2005; 280: 22670–8.

McMahon HT, Missler M, Li C, Südhof TC. Complexins: cytosolic proteins that regulate SNAP receptor function. Cell 1995; 83: 111–9.

Magnani E. Molecular physiology and pathology of tau protein interactions. PhD thesis. University of Cambridge, 2006.

Mangiarini L, Sathasivam K, Seller M, Cozens B, Harper A, Hetherington C, et al. Exon 1 of the HD gene with an expanded CAG repeat is sufficient to cause a progressive neurological phenotype in transgenic mice. Cell 1996; 87: 493–506.

Orimo S, Uchihara T, Nakamura A, Mori F, Kakita A, Wakabayashi K, et al. Axonal α-synuclein aggregates herald centripetal degeneration of cardiac sympathetic nerve in Parkinson's disease. Brain 2008; 131: 642–50.

Paxinos G, Franklin K. The mouse brain in stereotaxic coordinates. San Diego: Academic Press; 2001.

Periquet M, Fulga T, Myllykangas L, Schlossmacher MG, Feany MB. Aggregated α-synuclein mediates dopaminergic neurotoxicity *in vivo*. J Neurosci 2007; 27: 3338–46.

Polymeropoulos MH, Lavedan C, Leroy E, Ide SE, Dehejia A, Dutra A, et al. Mutation in α-synuclein gene identified in families with Parkinson's disease. Science 1997; 276: 2045–7.

Selkoe DJ. Alzheimer's disease is a synaptic failure. Science 2002; 298: 789–91.

Serpell LC, Berriman J, Jakes R, Goedert M, Crowther RA. Fiber diffraction of synthetic α-synuclein filaments shows amyloid-like cross-β conformation. Proc Natl Acad Sci USA 2000; 97: 4897–902.

Sidhu A, Wersinger C, Vernier P. Does α-synuclein modulate dopaminergic synaptic content and tone at the synapse? FASEB J 2004; 18: 637–47.

Singleton AB, Farrer M, Johnson J, Singleton A, Hague S, Kachergus J, et al. alpha-Synuclein locus triplication causes Parkinson's disease. Science 2003; 302: 841.

Specht CG, Schoepfer R. Deletion of the alpha-synuclein locus in a subpopulation of C57BL/6J inbred mice. BMC Neurosci 2001; 2: 11–19.

Spillantini MG, Speretta E, Goedert M, Magnani E. Tau and alpha-synuclein interaction in neurodegenerative diseases. Neurodeg Dis 2007; 4 (Suppl 1): 185.

Spillantini MG, Crowther RA, Jakes R, Hasegawa M, Goedert M. α-Synuclein in filamentous inclusions of Lewy bodies from Parkinson's disease and dementia with Lewy bodies. Proc Natl Acad Sci USA 1998; 95: 6469–73.

Spillantini MG, Schmidt ML, Lee VM-Y, Trojanowski JQ, Jakes R, Goedert M. α-Synuclein in Lewy bodies. Nature 1997; 338: 839–40.

Tofaris GK, Razzaq A, Ghetti B, Lilley KS, Spillantini MG. Ubiquitination of α-synuclein in Lewy bodies is a pathological event not associated with impairment of proteasome function. J Biol Chem 2003; 278: 44405–11.

Tofaris GK, Reitböck PG, Humby T, Lambourne SL, O'Connell M, Ghetti B, et al. Pathological changes in dopaminergic neurons in mice transgenic for human α-synuclein (1-120): implications for Lewy body disorders. J Neurosci 2006; 26: 3942–50.

Zarranz JJ, Alegre J, Gomez-Esteban JC, Lezcano E, Ros R, Ampuero I, et al. The new mutation E46K of α-synuclein causes Parkinson and Lewy body dementia. Ann Neurol 2004; 55: 164–73.

Zhou C, Huang Y, Przedborski S. Oxidative stress in Parkinson's disease. A mechanism of pathogenic and therapeutic significance. Ann NY Acad Sci 2008; 1147: 93–104.